

Intermodal Interference in Four-Mode Air-Silica Microstructure Fiber

Ji Yuling^{[a],*}; XU Peng^[a]

^[a]School of Physics and Information Engineering, Shanxi Normal University, Linfen, China.

*Corresponding author.

Supported by Shanxi Province Postgraduate Education Reform Project (104018).

Received 28 May 2015; accepted 18 August 2015
 Published online 26 September 2015

Abstract

Intermodal interference pattern along the fiber core has been observed when a properly femtosecond pulse is coupled into the four modes air-silica microstructure fibers. The interference pattern is well explained by using the modified effective refraction index model.

Key words: Intermode; Interference; Microstructure fiber

Ji, Y. L., & Xu, P. (2015). Intermodal Interference in Four-Mode Air-Silica Microstructure Fiber. *Advances in Natural Science*, 8(3), 6-9. Available from: <http://www.cscanada.net/index.php/ans/article/view/7727>
 DOI: <http://dx.doi.org/10.3968/7727>

INTRODUCTION

Intermodal interference in dual-mode or few-mode traditional fibers has been widely investigated, largely for its application in interferometric fiber-optic sensors (Sharma & Posey, 1996; Kumar, Jindal, Varshney, & Sangeet, 2000; Hentschel & Vojta, 2001; Hlubina, 2002; Mortensen, Stach, Broeng, Petersson, Simonsen, & Michalzik, 2003; Martin, 2004; Hlubina, 2005; Kisevetter, 2008). The performances of the interferometer systems are dominated by the group delay difference and the phase delay difference between the modes. However, the dispersion properties of traditional fiber cannot be tailed flexibly. Air-silica microstructured fibers (abbreviated as ASMF) (often called photonic crystal

fiber) have attracted significant attention because of their tailorable properties. ASMF commonly consists of a fused-silica core surrounded by a regular array of microscopic air holes along the entire fiber length. ASMF are currently the subject of intense research since they exhibit a variety of novel dispersive and nonlinear properties. All these characteristics result from the special microstructure of the two dimensions photonic crystal cladding. The novel cladding structure consisting of an array of micrometer-sized air holes allows for a very flexible tailoring of the dispersion curve. One can easily tailor the fibers to meet specific experimental needs by modifying the core size, the size and spacing of the air holes.

Modes and intermodal interference in ASMF have also been discussed lately (Ren, Wang, Lou, & Jian, 2003; Gu et al., 2003; Káčk, Martinček, Canning, & Lyytikäinen, 2004; Sugimoto, Nakamura, Tanaka, Ikeda, & Asakawa, 2005; Jin, Wang, & Ju, 2005; Wang, Ju, & Jin, 2006; Shih et al., 2004). In this paper, we report what we believe to be the first demonstration of four intermodal interference phenomena in four modes microstructure fibers.

1. EXPERIMENT

Our ASMF consist of a 0.85 μm radius silica core surrounded by an array of 0.45 μm radius air holes in a hexagonal close-packed arrangement. The center-to-center distance between the air holes (ditch) is 1.2 μm . An SEM image of a cleaved cross-section of the ASMF is shown in Figure 1. A pulse generated by the Ti: Sapphire laser is coupled into the ASMF. After a short distance propagation, a broadband spectrum (so-called supercontinuum spectrum) will be generated in the ASMF by self-phase modulation (SPM), stimulated Raman scattering (SRS), and parametric four-wave mixing (FWM) (Anton, Husakou, & Herrmann, 2002). Calculation shows that there are and there are only four guided modes (LP_{01} , LP_{11} ,

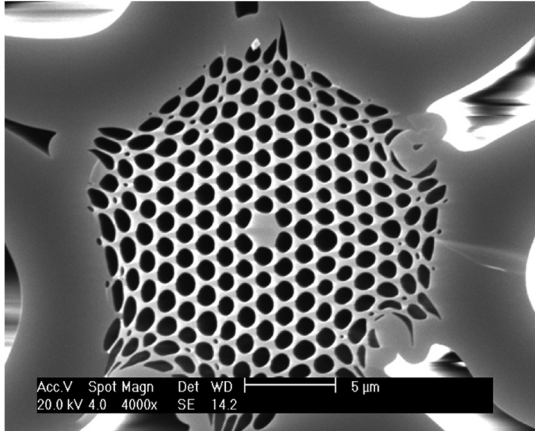


Figure 1
Cross-Section of the ASMf

LP_{21} , and LP_{02}) in the ASMf. Different modes of light have different propagation velocities along the fiber core. The lights which have the same wavelength in different modes will interfere when they meet in the fiber. Four-mode interference phenomena have been observed in the experiment. The four-mode interference picture in the ASMf is shown in Figure 2.

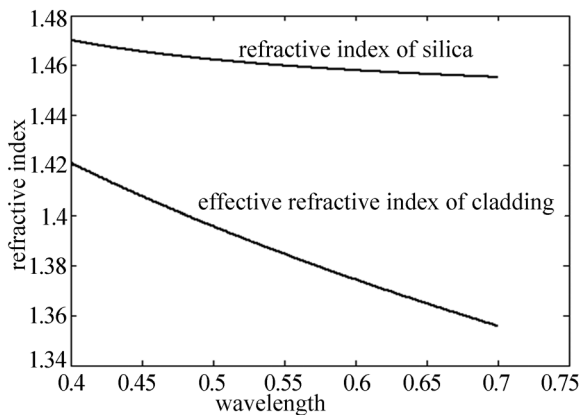


Figure 3
Effective Index of Cladding

Figure 3 shows the effective index of the cladding. For the convenience of comparison, the refractive index of silica is also given. Calculation shows that there are and there are only four guided modes existing in the ASMf we used. Figure 4 shows four guided modes' longitudinal propagation constants as the functions of wavelength. The light of the same frequency in the four modes will interfere with the process of propagation. Let us assume that there is the same fraction of the four-mode light for simple. The total light intensity at certain wavelength in the fiber should be:

$$|E|^2 = |E_1 + E_2 + E_3 + E_4|^2 = |a_1 e^{i\beta_1(\lambda)z} + a_2 e^{i\beta_2(\lambda)z} + a_3 e^{i\beta_3(\lambda)z} + a_4 e^{i\beta_4(\lambda)z}|^2$$

Here $\beta_i(\lambda)$ is the longitudinal propagation constant of the i^{th} mode.

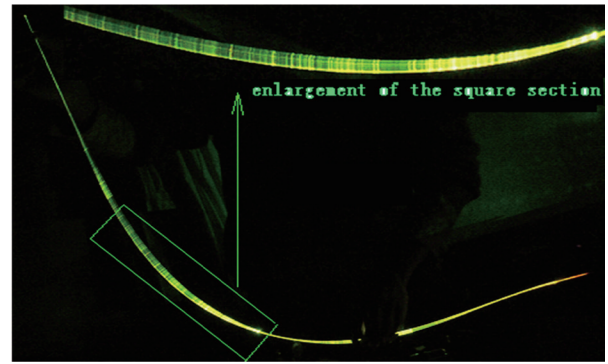


Figure 2
Four-Mode Interference Picture in ASMf

2. FOUR MODES INTERFERENCE THEORY

To study the interference phenomena of different modes in multimode fiber, we need a model for ASMf waveguide contribution to longitude propagation constants, which are calculated by the following two-step procedure (Anton, Husakou, & Herrmann, 2002). The cladding is considered as a two dimensions infinite large photonic crystal. ASMf is considered as a step-index fiber.

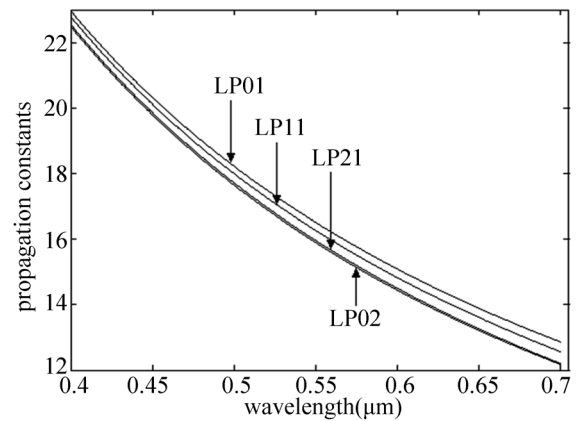


Figure 4
Propagation Constants of Different Modes

The intensity distributions along the fiber core at every wavelength values from $0.400\mu\text{m}$ to $0.700\mu\text{m}$, at a step of $2 \times 10^{-5}\mu\text{m}$, have been studied. We find that the intensity along the fiber core has a periodic maximum and minimum for every wavelength in some wavelength regions. After a more careful investigation, we found that the intensity of every wavelength has an obvious interference pattern along the fiber core in the following nineteen wavelength regions: $0.560156\text{-}0.560230\mu\text{m}$, $0.561182\text{-}0.561248\mu\text{m}$, $0.562206\text{-}0.562266\mu\text{m}$, $0.562714\text{-}0.562798\mu\text{m}$, $0.563752\text{-}0.563818\mu\text{m}$, $0.564786\text{-}0.564862\mu\text{m}$, $0.565316\text{-}0.565390\mu\text{m}$, $0.566342\text{-}0.566452\mu\text{m}$, $0.569032\text{-}0.569096\mu\text{m}$, $0.569560\text{-}0.569632\mu\text{m}$, $0.571170\text{-}0.571262\mu\text{m}$, $0.571736\text{-}0.571794\mu\text{m}$, $0.572818\text{-}0.572883\mu\text{m}$, $0.573367\text{-}0.573427\mu\text{m}$, $0.573916\text{-}0.574010\mu\text{m}$, 0.575030-

0.575094 μm , 0.575568-0.575648 μm , 0.576134-0.576198 μm , 0.578382-0.578456 μm . In these wavelength regions, the interference patterns are very sensitive to the wavelength changing. Figure 5 shows the interference patterns at wavelength 0.56483450 μm , 0.56483455 μm , 0.56483460 μm , 0.56483465 μm and 0.56483470 μm . For the other wavelength values which are not in these regions, the intensity distribution along the fiber core has no interference pattern at all.

Fortunately, the light propagation in the fiber is a super continuum spectrum. Naked eyes can not discriminate the color difference in a very small wavelength region. The visible result should be the intensity superimpose in a small wavelength region. Calculation shows that the superimpose intensity has similar interference pattern in any wavelength regions from 0.4 μm to 0.7 μm . Figure 6 shows the superimpose intensity distribution along the fiber core in wavelength regions 0.5890-0.5896 μm and 0.5796-0.5816 μm (superimpose step is $5 \times 10^{-7} \mu\text{m}$).

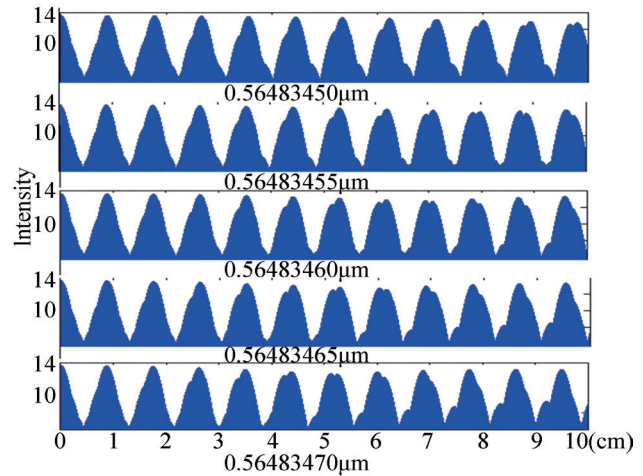


Figure 5
Intensity Distribution Along the Fiber Core at Special Wavelength Values

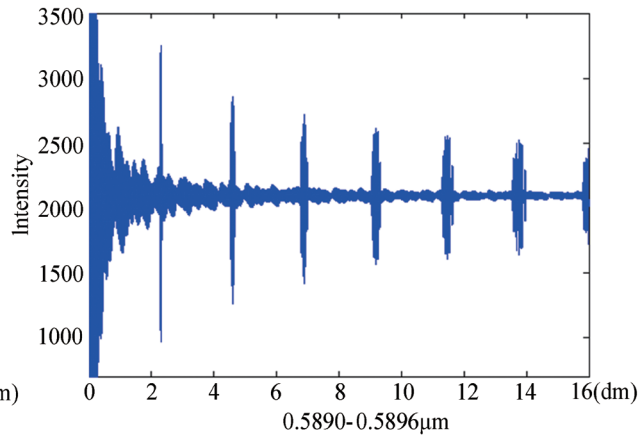
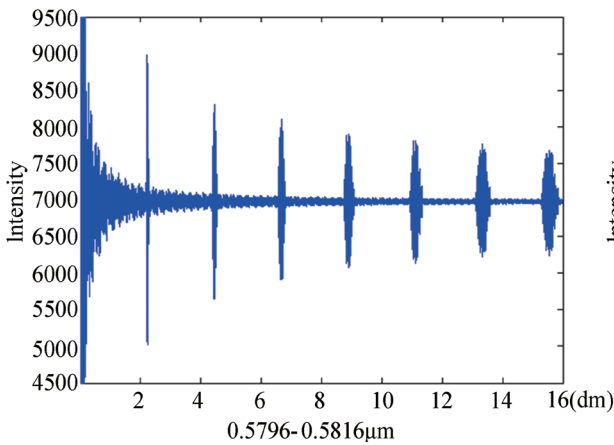


Figure 6
Superimpose Intensity in the Wavelength Regions 0.5890-0.5896 μm and 0.5796-0.5816 μm

Figure 7 is the intensity superimpose results in some wavelength regions (corresponding wavelength regions are 0.5000-0.5004 μm , 0.5250-0.5254 μm , 0.5506-0.5510 μm , 0.5750-0.5754 μm , 0.6000-0.6004 μm , 0.6250-0.6254 μm , 0.6500-0.6504 μm , 0.6750-0.6754 μm , 0.6990-0.6992 μm , superimpose step in every superimpose region is $5 \times 10^{-7} \mu\text{m}$). It is easy to notice that the superimpose interference patterns along the fiber core have a slight shift in different wavelength regions. From 0.5000 μm to 0.6992 μm , the first maximum series has a displacement shift of about 1.6dm. The second maximum series has a displacement shift of more than 3.2dm. The third maximum series has a displacement shift of about 5dm. The corresponding experimental result should be a series of interference maximum with a slight displacement shift and color difference. This agrees with the experimental result in Figure 2. We can imagine that if the spectrum is completely flat in the visible light wavelength region, the interference pattern should be a picture of continuous color changing.

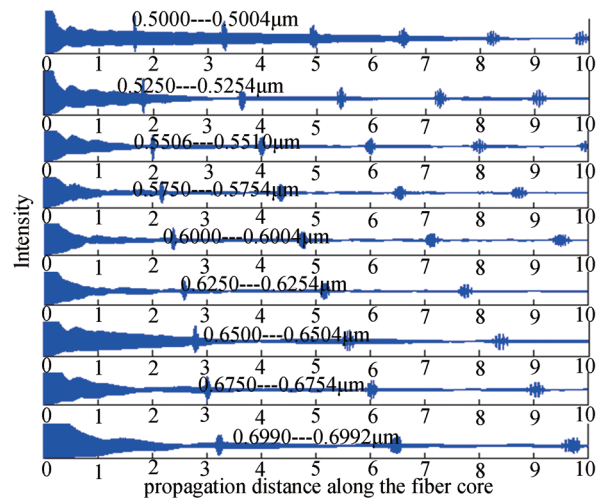


Figure 7
Intensity Distribution Along the Fiber Core in Some Wavelength Regions

DISCUSSION AND CONCLUSION

From the perspective of experiment, it is very difficult to get a completely flat supercontinuum. Some spikes always exist at some wavelength vicinity in the spectrum, and the superimpose intensity maximum in this wavelength vicinity will be enhanced. The four-mode interference phenomenon visible for naked eyes should be those enhanced interference maximum. So, the visible interference pattern and color of four-mode interference depend on where the spikes emerge in the supercontinuum. The color of interference maximums and the distance between the maximums varies with wavelength vicinities where the spikes emerged. From the color of the interference picture, we can know that Figure 2 is an interference picture of wavelength region from about $5,000\mu\text{m}$ to $6,000\mu\text{m}$. The spectrum has many spikes in this wavelength region, so we can see three series of interference maximums in a variety of colors. The first and the second maximum series are too compact for naked eyes to discriminate the neighboring maximums. The third maximum series is clear enough to be observed by naked eyes. This can be explained by Figure 7, the third maximum series displacement shift is larger than the first and the second maximum series shift in the wavelength region from $5,000\mu\text{m}$ to $6,000\mu\text{m}$. The fourth and higher maximum series overlaps with the next maximum series which produces a more complex interference pattern. Actually, due to the high loss of high order modes, the four-mode interference pattern will disappear after a long distance propagation. New long wavelength spectrum arises and the modes interference exist in this wavelength region within the short distance after the Ti:sapphire laser pulse is coupled into the ASMF. The enhanced long wavelength interference pattern could be observed. The enhanced shorter wavelength interference pattern will be observed after the propagation distance is increased and the new short wavelength spectrum arises.

Figure 8 is the interference picture in different supercontinuum conditions of the same ASMF. For a completely ideal flat supercontinuum spectrum, the interference distribution along the fiber core should be a continuous color changing.



Figure 8
Another Interference Picture

REFERENCES

- Husakou, A. V., & Herrmann, J. (2002). Supercontinuum generation, four-wave mixing, and fission of higher-order solitons in photonic-crystal fibers. *Journal of Optical Society of America B*, 19(9), 2171-2182.
- Káčik, D., Martinček, I., Canning, J., Issa, N. A., & Lyytikäinen, K. (2004). Intermodal interference in a photonic crystal fiber. *Optics Express*, 12(15), 3465-3471.
- Gu, X., Kimmel, M., Shreenath, A., Trebino, R., Dudley, J., Coen, S., & Windeler, R. (2003). Experimental studies of the coherence of microstructure-fiber supercontinuum. *Optics Express* 11, 2697-2703.
- Hentschel, M., & Vojta, M. (2001). Multiple beam interference in a quadrupolar glass fiber. *Optics Letter*, 26, 1764-1766.
- Hlubina, P. (2002). Spectral-domain intermodal interference under general measurement conditions. *Optics Communications*, 210(15), 225-232.
- Hlubina, P. (2005). Spectral-domain intermodal interference and the effect of a low-resolution spectrometer. *Optik*, 116, 469-474.
- Jin, W., Wang, Z., & Ju, J. (2005). Two mode photonic crystal fibers. *Optics Express*, 13, 2082-2088.
- Kisevetter, D. V. (2008). Quasi-ray description of intermode interference of the radiation of optical vortices in short fiber lightguides. *Journal of Optical Technology*, 75(1) 64-66.
- Kumar, A., Jindal, R., Varshney, R. K., & Sangeet, K. S. (2000). A fiber-optic temperature sensor based on LP_{01} - LP_{02} mode interference. *Optical Fiber Technology*, 6, 83-90.
- Martinček, M., Káčik I.T., & Peterka, P. (2004). The determination of the refractive index profile in α -profile optical fibres by intermodal interference investigation. *Optik*, 115(2), 86-88.
- Mortensen, N. A., Stach, M., Broeng, J., Petersson, A., Simonsen, H. R., & Michalzik, R. (2003, August 25). Multi-mode photonic crystal fibers for VCSEL based data transmission. *Optics Express*, 11(17), 1953-1959.
- Ren, G. B., Wang, Z., Lou S. Q., & Jian, S.S. (2003, June 2). Mode classification and degeneracy in photonic crystal fibers. *Optics Express*, 11(11), 1310-1321.
- Sharma, A., & Posey, R. (1996). Transverse stress induced LP_{02} - LP_{21} modal interference of stimulated Raman scattered light in a few-mode optical fiber. *Optics Communications*, 124, 111-117.
- Shih, M. H., Kim, W. J., Kuang, W., Cao, J. R., Yukawa, H., Choi, S. J., O'Brien, J. D., Dapkus, P. D., & Marshall, W. K. (2004). Two-dimensional photonic crystal Mach-Zehnder interferometers. *Appl. Phys. Lett.*, 84, 460-462.
- Sugimoto, Y., Nakamura, H., Tanaka, Y., Ikeda, N. & Asakawa, K. (2005, January 10). High-precision optical interference in Mach-Zehnder-type photonic crystal waveguide. *Optics Express*, 139(1), 96-105.
- Wang, Z., Ju, J., & Jin. W. (2006). Optimizing PCF for two-mode interference. *Optical Fiber Technology*, 12, 29-37.